Nonlinear dispersion in resonant Auger decay of H₂O molecules

M. N. Piancastelli,[1,*] B. Kempgens,[1] U. Hergenhahn,[1] A. Kivimäki,[2] K. Maier,[1] A. Rüdel,[1] and A. M. Bradshaw[1]

[1]*Fritz-Haber-Institut der Max-Planck-Gesellschaft, Faradayweg 4-6, 14195 Berlin, Germany*
[2]*Department of Physical Sciences, University of Oulu, 90570 Oulu, Finland*

We have measured the resonant Auger decay spectrum of the water molecule at the oxygen K edge. Strong deviations from the expected linear dispersion of the participator lines (which correspond to single-hole valence states) are observed. In a simplified picture the effect can be attributed to the combined effect of the intermediate- and final-state potential curves. [S1050-2947(99)09302-6]

PACS number(s): 33.80.Eh, 33.70.Jg, 33.60.−q

I. INTRODUCTION

The radiationless decay of core-excited molecules has recently been studied in several cases under conditions corresponding to the Auger equivalent of the resonant Raman effect [1–5]. The basic experimental feature is the measurement of electron decay spectra following the excitation to a particular resonant core state below the ionization threshold with a photon bandwidth significantly narrower than the natural linewidth of the resonance itself. In this way, it is possible to overcome the line broadening associated with the short lifetime of the resonant state and to observe spectral features that would otherwise be obscured. The main results reported to date have been line narrowing and linear energy dispersion in the decay spectra. Although these phenomena are expected from energy conservation, the interplay between the line shape of the photon band and the natural line shape of the resonant Auger lines has been shown to affect the spectra in a nontrivial way. The dispersion relation for the center of gravity of lines in the spectrum of an atom, for example, was considered both experimentally and theoretically by Kukk *et al.* [2]. Linear dispersion with a unit slope was found to be the limiting case for a narrow photon bandwidth, while in the general case symmetric deviations about such a straight line were observed. The dispersion relation for a molecular system will be more complicated, as energy can also be absorbed into vibrational degrees of freedom. Furthermore, the nature of the intermediate and final states (either bound or dissociative) has to be taken into account. For resonant x-ray scattering (both radiative and radiationless) from a bound molecular excited state Gel'mukhanov and Ågren [6] have predicted a wealth of phenomena, including the possibility of so-called anti-Raman dispersion, i.e., the center of gravity disperses with a negative slope. We then have the result that *increasing* the photon energy will *lower* the energy of the scattered photon or, in the present case, of the Auger decay line.

In this article we describe the participator decay spectra of water recorded at the O $1s$-$4a_1$ and O $1s$-$2b_2$ resonances

excited by a photon band much smaller than the resonant linewidth. (Participator processes involve the electron that has been excited and result in final states with a single hole in the valence shell. Spectator processes, where the excited electron is not involved, result in two-hole–one-electron final states at lower kinetic energy.) We measure the dispersion relationships for decay into the $1b_1^{-1}$, $3a_1^{-1}$, and $1b_2^{-1}$ final states and demonstrate strong, previously unobserved deviations from linear behavior.

II. EXPERIMENT

A. Experimental procedure

The decay spectra have been obtained on the X1B undulator beam line at the National Synchrotron Light Source, Brookhaven National Laboratory. The spherical grating monochromator and the angle-resolving cylindrical mirror electron energy analyzer (CMA) have been described in detail elsewhere [7]. The decay spectra following the O $1s$-$4a_1$ and O $1s$-$2b_2$ transitions have been recorded with 25/25-μm slits corresponding to a photon bandwidth of approximately 210 meV. This slit setting does not provide the best possible photon bandwidth (which would be approximately 100 meV with 5/5-μm slits), but has been chosen to achieve a reasonable compromise between resolution and measuring time. Since the absorption bands are very broad ($\approx$1 eV) and do not show any vibrational fine structure, the spectra could be recorded in rather large photon energy steps of 300 meV. The CMA was set at a pass energy of 80 eV, giving an electron energy resolution of 0.7 eV, again to increase the signal. All measurements were normalized with respect to photon flux and target gas pressure.

Electron decay spectra have been measured in the photon energy range 532.9–537.1 eV, which includes the three most intense below-threshold resonances at 534.1, 535.9, and 537.1 eV, assigned as transitions from the O $1s$ core level to the empty states $4a_1$, $2b_2$, and $2b_1$, respectively. The energy calibration has been made on the basis of electron-energy-loss spectroscopy measurements [8]. The photoabsorption curve has been reported in the literature and the spectral assignment made by comparison with calculated terms [9]. The first two states are assigned to a mixture of
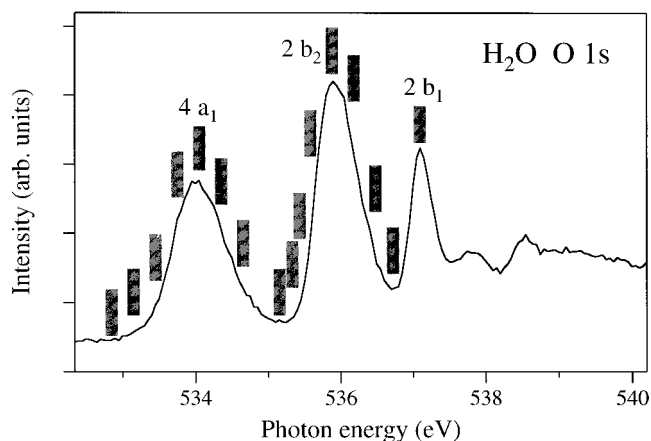
FIG. 1. O $1s$ photoabsorption curve of the water molecule measured in the partial electron yield mode. The three maxima correspond to the O $1s$-$4a_1$, O $1s$-$2b_2$, and O $1s$-$2b_1$ transitions, respectively. The vertical bars indicate the photon energy values at which decay spectra have been measured.

antibonding molecular orbitals and Rydberg states, while the third is a pure Rydberg state. In Fig. 1 we show an absorption curve obtained in the partial electron yield mode. The vertical bars indicate the photon energy values at which decay spectra were recorded. We plan to give a detailed description of the decay spectra including the spectator lines elsewhere [10].

B. Experimental results

Figures 2(a) and 2(b) show the participator $1b_1^{-1}$, $3a_1^{-1}$, and $1b_2^{-1}$ lines for three photon energies spanning the O $1s$-$4a_1$ transition [Fig. 2(a)] and the O $1s$-$2b_2$ transition [Fig. 2(b)]. These final states are also populated to some extent by direct photoionization, as can be seen from the nonvanishing intensity outside the resonances. The spectator lines at lower kinetic energy are not shown. The bold dashed lines highlight the relative shift in kinetic energy. There are some variations in the relative intensity of the peaks that are related to the symmetry coupling between intermediate and final states and will be discussed elsewhere [10]. Here we emphasize the deviations from linear dispersion. In particular, in Fig. 2(a) all three peaks remain initially at almost constant kinetic energy while the photon energy is changed by 600 meV but then disperse with a slope of unity when the photon energy is further increased. Whereas the $1b_1^{-1}$ feature in Fig. 2(b) also shows this "normal" behavior, i.e., its kinetic energy changes linearly with unit slope, the $1b_2^{-1}$ peak shows an increase in kinetic energy of 1.2 eV when the photon energy is increased by 430 meV, but then decreases in kinetic energy when the photon energy is further increased.

Plots of kinetic energy versus photon energy for all photon energies measured are shown in Fig. 3. The vertical error bars are set to ± 0.15 eV, largely due to the fact that kinetic-energy steps of 0.1 eV were used to record the spectra. Horizontal error bars due to thermal drift are negligible with respect to the photon energy steps used. The values of the kinetic energy at the peak centers have been obtained by a fitting procedure using three symmetric Gaussians for the
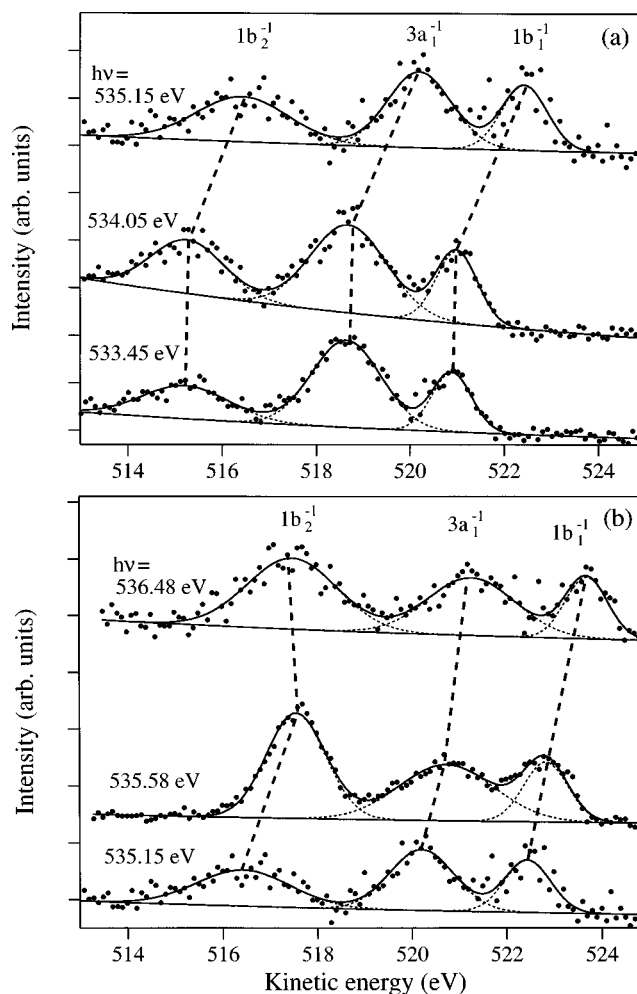

FIG. 2. Decay spectra (points) measured in the photon energy ranges of the (a) O $1s$-$4a_1$ and (b) O $1s$-$2b_2$ excitations. The solid lines represent the result of a least-squares fit of three symmetric Gaussians to the experimental data. The bold dashed lines are a guide to the eye connecting peak maxima at different photon energies.

three participator lines. Although the participator lines might exhibit an asymmetry resulting from their vibrational envelopes, these effects are obviously too small to be significant in our spectra. The straight lines are not fits to the experimental points, but rather connect the first and last points in each plot. In all these cases, their slope turns out to be unity, as expected for photon energies where there are no resonant transitions into valence states.

We notice that the $1b_1^{-1}$ state exhibits almost linear energy dispersion with unit slope over the whole photon energy range, but with a weak deviation near the photon energy region of the O $1s$-$4a_1$ resonance. The situation is quite different for the $3a_1^{-1}$ and the $1b_2^{-1}$ states, for which there is a marked deviation from linear dispersion in the photon energy ranges corresponding to the O $1s$-$4a_1$ and O $1s$-$2b_2$ transitions. In particular, we note that for the $1b_2^{-1}$ participator line there is even a region of dispersion with a slope greater than unity followed by one with negative slope, i.e., in the latter case, increasing the photon energy gives rise to a decrease in the energy of the decay line. We checked the possibility that the deviations from unit slope were due to the
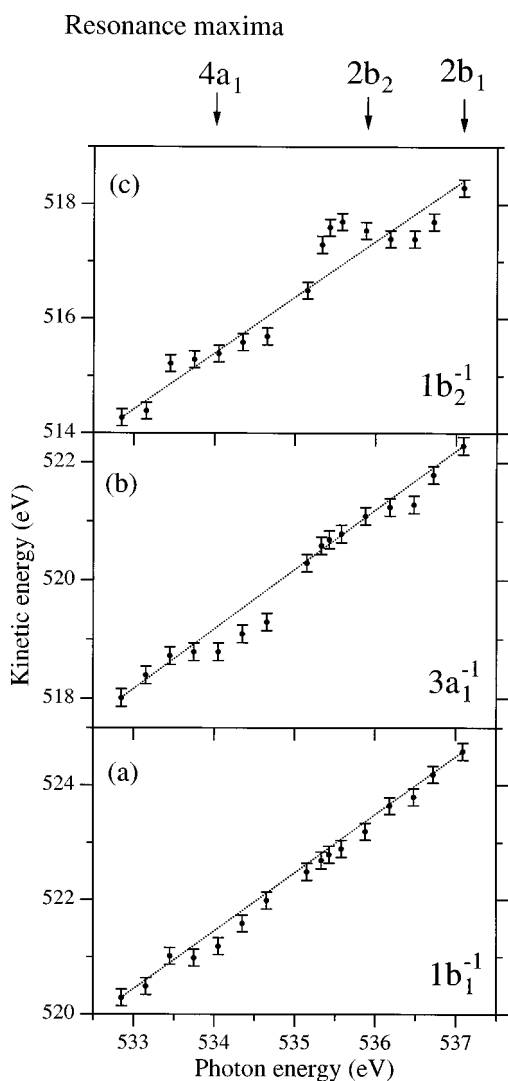
Resonance maxima

FIG. 3. Dispersion curves for the three participator lines corresponding to the (a) $1b_1^{-1}$, (b) $3a_1^{-1}$, and (c) $1b_2^{-1}$ final states. The straight lines connect the first and last data points in each plot, corresponding to linear dispersion with unit slope.

apparatus by performing a numerical simulation in the spirit of Kukk *et al.* [2]. Symmetric deviations about the diagonal by about 250 meV maximum amplitude were found, which can contribute, but are not sufficient, to explain our observations.

On examining the appearance of the absorption features in Fig. 1 we note that there is no resolved vibrational fine structure, as has been reported several times in the literature for both isolated and condensed water molecules; see e.g., [9,11]. Schirmer *et al.* [9] remark that both states are likely to be dissociative on the basis of their calculations. Ultrafast dissociation following the O $1s$-$4a_1$ excitation has in fact been suggested from H$^+$ yield measurements on condensed water [11,12]. Some evidence as to the nature of these core-excited states can also be obtained by analogy with valence-excited H$_2$O. The features can be compared to the $\tilde{A}$ $^1B_1$ state corresponding to excitation of a nonbonding $1b_1$ electron into the $4a_1$ level and to the dipole-forbidden excitation into the $(1b_1^{-1}2b_2)$ $^1A_2$ state. Potential curves of these states have been calculated using configuration-interaction methods

[13]. The main findings are that the $\tilde{A}$ state is unstable along the asymmetric stretch coordinate, while the $^1A_2$ state has bound potential curves for symmetric and asymmetric bond elongation. Bond angles are similar to the ground state in both cases. We might thus expect the first core-excited state to decay by hydrogen abstraction, possibly on a time scale that is comparable to electronic decay. The geometries of the first three ionic states of water have also been calculated using *ab initio* methods [14]. Strong changes in geometry are expected for the $3a_1^{-1}$ and $1b_2^{-1}$ states, the first one being linear and the other bent to 55.7° (compared to 104.5° in the ground state). A bond elongation by about 0.13 Å is also predicted for the $1b_2^{-1}$ state.

III. INTERPRETATION

We now turn our attention to possible explanations for the observed nonlinear dispersion effects. As the shape of all three participator lines will be determined by the unresolved vibrational envelopes, changes in the degree of vibrational excitation while tuning through the resonance could give rise to a change in the center of gravity. One phenomenon that is known to influence the final-state vibrational distribution is lifetime-vibrational interference (LVI) (see, e.g., [15]). We attempt to make plausible below, however, that the occurrence of LVI is not necessary, at least not for a shift in the center of gravity to occur. Additionally, in the case of a dissociative intermediate state, electronic decay and nuclear motion might take place on similar time scales. A time-dependent treatment of the electronic decay on the repulsive potential-energy surface would then be necessary; in this situation any kind of energy exchange between the nuclear and electronic degrees of freedom is conceivable. Although an explanation in these terms might describe completely the present phenomenon, this treatment is clearly beyond the scope of this article. We will therefore explore some recent ideas from time-independent scattering theory to show that there are possible mechanisms giving rise to nonlinear dispersion of participator Auger lines for the cases of both bound and dissociative intermediate states.

Resonant x-ray scattering with a bound ground state, a dissociative intermediate state, and a bound final state (bound-continuum-bound or *bcb* transitions) have recently been considered by Gel'mukhanov and Ågren [16]. These results can be applied to resonant Auger decay as well. A main finding is that the excitation probability to the intermediate state as a function of energy resembles the shape of the ground-state vibrational wave function in real space, a result that has already been shown less rigorously by Herzberg [17]. This is because the maximum excitation probability corresponds to the energy of the vertical transition from the ground-state equilibrium point. The excitation probability at other ground-state configurations will peak at other excitation energies since the slope of the intermediate-state potential also leads to differences between the potential curves at these points. Thus differences in the spatial coordinates are mapped to differences in energy and further to differences in excitation probability. If we assume the evolution time on the potential surface to be short compared to the electronic decay time, the same mechanism will apply to decay. Stated in terms of energies, this requirement means that the effec-
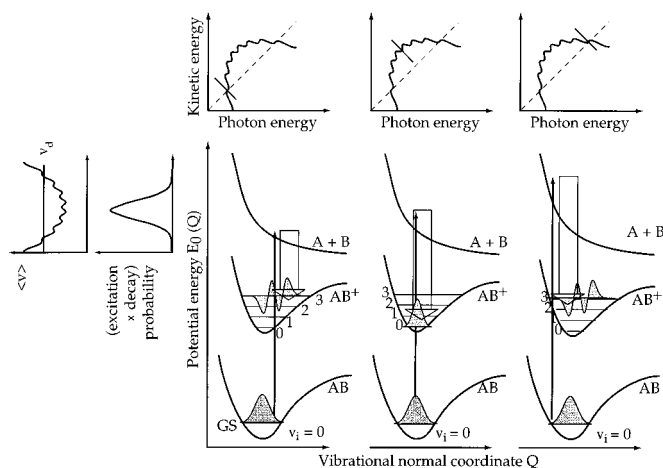
FIG. 4. Sketches of the possible interplay between the potential curves of a dissociative intermediate state and a bound final state. Two left insets: excitation probability and average vibrational quantum number $\langle v \rangle$ for the ''excitation-times-decay'' probability. $\langle v \rangle$ must be compared with the average vibrational quantum number v_d of the direct transitions (straight line in the plot of $\langle v \rangle$). Top insets: linear dispersion curve (dashed) and effects expected from resonant vibrational quanta distribution (solid). In an exact picture, the solid curve would join smoothly with the dashed one at the edges of the depicted region due to the effect of the direct transition probability.

tive width of the resonance should be broad compared to the lifetime broadening. The (*bcb*) scattering probability is then proportional to the square of the product of two harmonic-oscillator functions, multiplied by the photon bandpass for energy conservation. Nonlinear dispersion is possible, and even probable, because harmonic-oscillator wave functions of higher quantum number v have their maximum amplitude further away from the equilibrium position. For strong detuning from the vertical frequency, the decay probability to higher vibrational levels is then enhanced, which in turn reduces the emitted electron energy. The situation is sketched in Fig. 4, which highlights that deviations from linear dispersion similar to the ones observed here are possible by that mechanism. Strong effects are expected for a shallow (weakly dissociating) intermediate-state potential curve and for a large spacing of the final-state vibrational levels.

Even this explanation might not be completely sufficient since water is a polyatomic molecule with three vibrational normal coordinates: It can decay along one normal coordinate, but be perfectly stable with respect to the other two. This implies that, in the case of excitation of one of the stable modes in the final state, the problem must indeed be seen as a scattering process via a *bound* intermediate state. Applying the theory for bound-bound resonant x-ray scattering (*bbb* transitions) [6], the slope of the dispersion curve would, in a first approximation, be dependent on the difference in the intermediate- and final-state vibrational energies. Anomalous dispersion is again possible for intermediate final states having vibrational spacings much smaller than in the final state [6].

We now briefly discuss the results in Fig. 3 in the light of these models. The $1b_1^{-1}$ participator line seems to show linear dispersion of unit slope within the limits of the experimental error over the whole range investigated [Fig. 3(a)]. This can be tentatively explained by the nature of this state:

It is mainly localized on the oxygen atom with lone-pair character, while the other two participator lines are related to the two bonding O-H orbitals. We can therefore assume that the $1b_1^{-1}$ state couples least effectively to the resonances, so that *bcb* transitions are unimportant compared to direct transitions. As the geometry changes along the transition path are also small, no obvious mechanism for strong vibrational excitations via *bbb* transitions exists as well. The behavior of the other two lines is more complex. On the $4a_1$ resonance a nearly vanishing slope is observed for both. Since the latter is most likely to be dissociative, this could provide an example for the *bcb* transition path. However, for very fast dissociation a background signal from decay events between the dissociative parts of the potential curves should be observable. No such features seem to be obvious in the spectra. This conforms with the notion that dissociative forces in the $4a_1$ excited state are indeed not so large, a fact that leads to the anomalous dispersion. There is no shift of the potential curves between the ground and final states along the antisymmetric stretching coordinate [14]. Detuning away from the resonance should thus sample different regions of the potential curves and lead to higher vibrational excitations, in analogy to examples for lifetime vibrational interference [15].

For the $2b_2$ resonance decaying to the $1b_2^{-1}$ state, the anomalous dispersion is strongest. Under the assumption of a bound intermediate state, the relation between the appropriate vibrational frequencies and the experimentally observed slope given in [6] can be invoked. Using 372 meV [14] for the $1b_2^{-1}$ state, we arrive at 245 meV for the $2b_2/3p$ excited state. This conforms with the expectation of a relatively weakly bound-state potential curve. However, if we assume the lifetime broadening of the resonance to be 150 meV, identical to that of the O $1s$ hole state in H_2O [18], then the vibrational fine structure would have been visible in the absorption spectra of Schirmer *et al.* [9] without an additional broadening mechanism.

IV. CONCLUSION

In conclusion, we present in this paper spectra showing strong deviations from linear energy dispersion of features in the decay spectrum of the core-excited states of the water molecule. The effect cannot be explained alone by the convolution of the photon band and the line shape of the resonances [2]. Rather, it is attributed either to the presence of dissociation taking place on the same time scale as the electronic decay or to the interplay of the intermediate state with the bound initial and final states. In the first case, the change in slope of the dispersion curve can be related to an energy partitioning between the outgoing electron and the H atom or proton, which begins to move simultaneously with electronic decay. In the second case, it would be due to the varying energy separation between the intermediate state and the final states, as different regions of the potential-energy curves are probed by the absorption process. It is also possible that both effects occur. The latter model can be related to recent theoretical results on radiative x-ray scattering [6,16], which, strongly simplified, state that anomalous dispersion effects are possible for intermediate states having shallow potential curves compared to the final state.

[1] M. N. Piancastelli, M. Neeb, A. Kivimäki, B. Kempgens, H. M. Köppe, K. Maier, and A. M. Bradshaw, Phys. Rev. Lett. **77**, 4302 (1996), and references therein.

[2] E. Kukk, S. Aksela, and H. Aksela, Phys. Rev. A **53**, 3271 (1996), and references therein.

[3] A. Kivimäki, A. Naves de Brito, S. Aksela, H. Aksela, O.-P. Sairanen, A. Ausmees, S. J. Osborne, L. B. Dantas, and S. Svensson, Phys. Rev. Lett. **71**, 4307 (1993).

[4] Z. F. Liu, G. M. Bancroft, K. H. Tan, and M. Schachter, Phys. Rev. Lett. **72**, 621 (1994).

[5] R. Camilloni, M. Zitnik, C. Comicioli, K. C. Prince, M. Zacchigna, C. Crotti, C. Ottaviani, C. Quaresima, P. Perfetti, and G. Stefani, Phys. Rev. Lett. **77**, 2646 (1996).

[6] F. Gel'mukhanov and H. Ågren, Phys. Rev. A **54**, 3960 (1996).

[7] K. J. Randall, J. Feldhaus, W. Erlebach, A. M. Bradshaw, Z. Xu, Y. Ma, and P. D. Johnson, Rev. Sci. Instrum. **63**, 1367 (1992); J. Feldhaus, W. Erlebach, A. L. D. Kilcoyne, K. J. Randall, and M. Schmidbauer, *ibid.* **63**, 1454 (1992).

[8] G. R. Wight and C. Brion, J. Electron Spectrosc. Relat. Phenom. **4**, 25 (1974).

[9] J. Schirmer, A. B. Trofimov, K. J. Randall, J. Feldhaus, A. M. Bradshaw, Y. Ma, C. T. Chen, and F. Sette, Phys. Rev. A **47**, 1136 (1993).

[10] M. N. Piancastelli, B. Kempgens, A. Kivimäki, K. Maier, U. Hergenhahn, A. Rüdel, and A. M. Bradshaw (unpublished).

[11] D. Coulman, A. Puschmann, U. Höfer, H.-P. Steinrück, W. Wurth, P. Feulner, and D. Menzel, J. Chem. Phys. **93**, 58 (1990), and references therein.

[12] K. Mase, M. Nagasono, S. Tanaka, T. Urisu, E. Ikenaga, T. Sekitani, and K. Tanaka, J. Chem. Phys. **108**, 6550 (1998).

[13] G. Theodorakopoulos, I. D. Petsalakis, R. J. Buenker, and S. D. Peyerimhoff, Chem. Phys. Lett. **105**, 253 (1984); G. Theodorakopoulos, I. D. Petsalakis, and R. J. Buenker, Chem. Phys. **96**, 217 (1985).

[14] C. F. Jackels, J. Chem. Phys. **72**, 4873 (1980).

[15] T. X. Carroll, S. E. Anderson, L. Ungier, and T. D. Thomas, Phys. Rev. Lett. **58**, 867 (1987); W. Eberhardt, J.-E. Rubensson, K. J. Randall, J. Feldhaus, A. L. D. Kilcoyne, A. M. Bradshaw, Z. Xu, P. D. Johnson, and Y. Ma, Phys. Scr. **T41**, 143 (1992); M. Neeb, J.-E. Rubensson, M. Biermann, and W. Eberhardt, J. Electron Spectrosc. Relat. Phenom. **67**, 261 (1994).

[16] F. Gel'mukhanov and H. Ågren, Phys. Rev. A **54**, 379 (1996).

[17] G. Herzberg, *Molecular Spectra and Molecular Structure, 1: Spectra of Diatomic Molecules* (Van Nostrand Reinhold, New York, 1950), p. 175.

[18] A. Cesar, H. Ågren, and V. Carravetta, Phys. Rev. A **40**, 187 (1989).